PERGAMON

Electrochimica Acta 44 (1999) 2859–2870

ELECTROCHIMICA Acta

Pulse current plating of TiB_2 in molten fluoride

Gerhard Ett, Elisabete J. Pessine *

Molten Salt Group, Materials Engineering Department, Nuclear and Energy Research Institute, IPEN, C.P. 11049, 05422-970 São Paulo, SP, Brazil

Received 26 August 1998; received in revised form 20 November 1998

Abstract

The investigation of TiB_2 electrodeposition was carried out using continuous current plating (CCP) and pulse current plating (PCP), electrochemical techniques to produce a uniform and a very low porosity coating. The solvent used is a fluoride mixture (LiF–NaF–KF) with solutes K_2TiF_6 and KBG_4 in a mass relation of one to four after treatment to remove moisture. The temperature was 600°C and all results were obtained on graphite electrodes as substrate. When necessary, the working electrode potentials were monitored with a $Ni/Ni^{2+}//BN$ reference electrode.

The electrodeposition with pulse current plating produces coatings with better quality, showing fewer cracks and better adhesion to the substrate and no anode effect was observed, when compared with those obtained by continuous current plating, for the conditions: frequencies between 5–100 Hz, t_c/t_{off} between 5/1–3/1 or i_c/i_{off} between 1.5 and 1.8.

Keywords: Titanium diboride; Pulse plating; Molten salts; Flinak; Electrodeposition

1. Introduction

The titanium diboride presents as special properties [1]: high hardness (3350 $Hv)_{0.5N}$, high melting point (2980°C), low electrical resistivity (9 μΩ cm), good absorption cross section for thermal neutrons (1524 barns), high wettability and good thermal shock resistance.

Furthermore, it has the property to resist the attack of molten metals, HF, HCl and of molten salts; however, it dissolves in H_2SO_4 and in mixtures of $HNO_3 + H_2O_2$ or $HNO_3 + H_2SO_4$.

Due to these properties, it is well suited for coating on electrodes, turbine blades, combustion chambers, chemical reactor vessels, crucibles, pump impellers, protective shields for thermocouples and cutting tools.

There are several procedures available for the preparation of borides, but always at high temperatures. Those most used in industry are the following:

1. synthesis from the elements B and Ti or from B and a hydride of the metal,
2. chemical vapor deposition (CVD),
3. aluminothermy,
4. reduction of the metal oxide with $B_4C + C$ and
5. electrolysis from a mixture of molten salts.

The electrolysis from molten salts media has, however, shown to be quite efficient in the preparation of deposits that are not only adherent, but as free of pores and of impurities.

Andrieux [2], in 1929, considered the precursor of the electrochemical preparation of TiB_2, in molten salts medium, prepared on Inconel and graphite substrates, countless different compositions of borides

* Corresponding author. Fax: +55-11-816-9370; e-mail: epessine@net.ipen.br

0013-4686/99/$ - see front matter
PII: S0013-4686(98)00402-2

from two electrolytic mixtures, e.g. MgO, MgF_2, $2B_2O_3$, $\frac{1}{2}TiO_2$ and CaO, CaF_2, $2B_2O_3$, $\frac{1}{4}TiO_2$, at 750°C.

Schlain, McCawley and Smith [3], in 1969, used a mixture of $NaBO_2 + LiBO_2 + Na2TiO_3 + TiO_2$ at 900°C, using copper as substrate. After 3 years of continuous work, they obtained adherent deposits, hard and brilliant and patented the procedure.

Giess [4], in 1972 and Kellner [5], in 1973, patented a preparation in which the electrolyte was constituted by mixtures of LiF–KF–KBF_4–TiF_3 and of LiF–KF–BF_3–TiF_3 at 900°C. Three years latter Gomes, Uchida and Wong [6] produced deposits with 98% of purity, in the medium of $Na_2B_4O_7$–Na_2CO_3–Na_3AlF_6–NaCl–TiO_2 at 1025°C.

Makyta, Gjortheim and Matiasovský [7], in 1988, consolidated the K_2TiF_6 as solute and the KF_4 and the mixtures of fluorides, LiF–KCl and KF–KCl as solvent at 750°C. The results presented involved the fundamental aspects of electrochemical kinetics [8], as well as several tests aimed at the improvement of the preparation process of coatings on some substrates. Nearly at the same time, Wendt et al. [9, 10], in 1989 and 1991

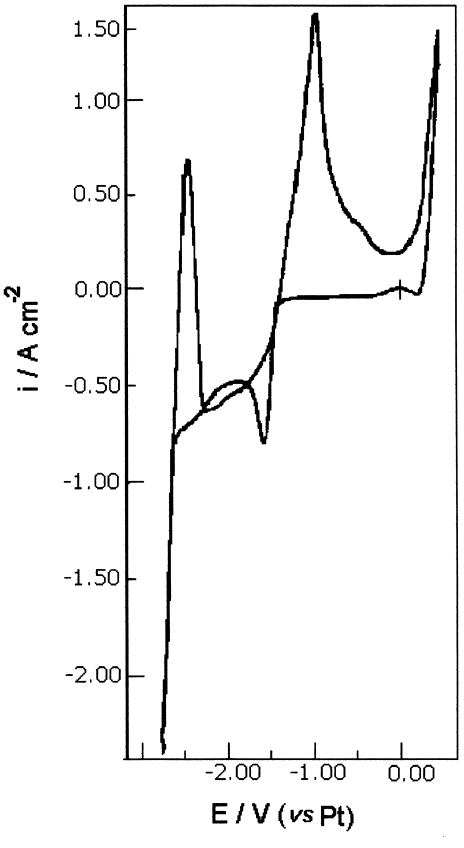

Fig. 1. Cyclic Voltammogram of TiB_2. $\upsilon = 200$ mV/s, 600°C, $B^{3+}/Ti^{4+} = 4/1$ on copper electrode.

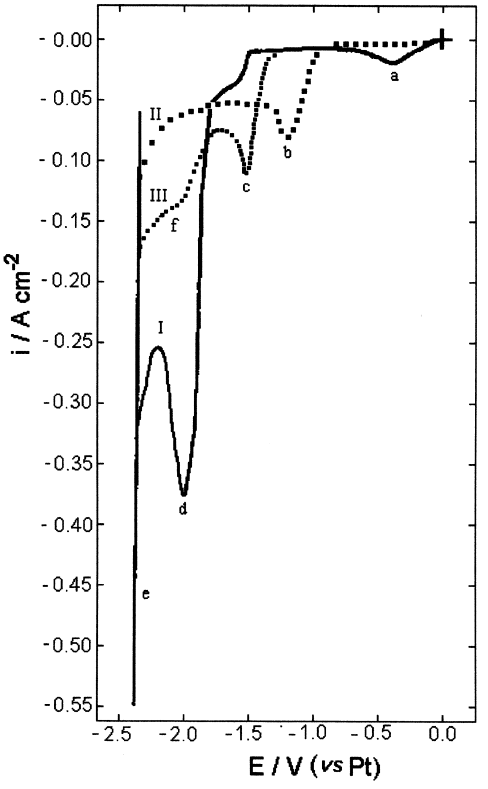

Fig. 2. Cyclic voltammograms of TiB_2. $\upsilon = 200$ mV/s, 600°C. Curves: (I) 0.5 mol/L K_2TiF_6, (II) 1 mol/L KBF_4 and (III) 0.5 mol/L K_2TiF_6 + 1 mol/L KBF_4 and Pt-working electrode.

published two complete papers in which they described the electrochemical behavior and the electrodeposition in fluoride media on copper substrates.

New results were published between 1992 and 1996 by Makyta's group [11], all of them aiming at the optimization of the preparation process of TiB_2 coatings, changing the electrolyte mixture or the experimental technique. There are several specific molten electrolytes to prepare TiB_2 coatings with low contents of contamination. The most frequently used are: chlorides and/or fluorides, cryolite and oxides mixtures. Among these electrolytes, the ones with fluorides, chlorides and the mixtures of fluorides + chlorides give the best deposits. The chloride electrolytes present some advantages in relation to the fluorides: they are cheaper, less corrosive to the materials used in the apparatus and the salt is more easily removed from the deposits. However, the electrolytes composed by mixtures of fluorides have been the most used for they allow thicker coatings and better yield.

Previous studies have applied continuous current plating; to the deposition of TiB_2 the aim of the present work is to compare the coating qualities of TiB_2

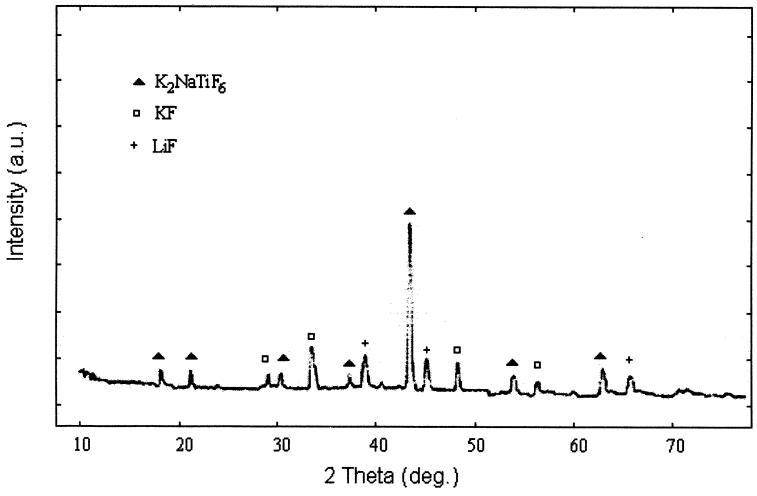

Fig. 3. The X-ray diffraction analysis of deposit over graphite from Flinak-1 mol/L K_2TiF_6 electrolyte.

prepared by electrodeposition by continuous current and by pulse current plating.

2. Experimental

The solvent used in the electrodeposition was an eutectic Flinak mixture (LiF–NaF–KF, 46.5–11.5–42 mol%) (m.p. = 454°C and $\rho = 1.96$ g cm^{-3} (700°C) and the solute used was a mixture of K_2TiF_6 and KBF_4 in the concentration ratio of 1:4.

Impurities such as H^+, OH^-, H_2O and O^{2-} in the electrolyte are undesirable because they interfere with the quality of the electroplating, promote corrosion of the apparatus and allow some undesirable electrochemical reactions. Therefore, the electrolyte has to be dehydrated at 140°C for 48 h under vacuum in order to eliminate the water present in KF. After homogenization the melt was introduced into a high purity graphite crucible placed in the interior of an electrolytic reactor [12].

The temperature used in this study was 600°C, because in thermogravimetric tests it was observed that at higher temperatures an accentuated decrease of the yield occurs, due to the evaporation of KBF_4 in the form of BF_3.

The working electrode was graphite, because it has a thermal expansion coefficient (4.3 μm/cm °C) close to the TiB_2 (4.6 μm/cm °C). A platinum wire was used as a pseudo reference electrode and when necessary a Ni/Ni^{2+}//BN reference electrode [13] was used during the deposition experiments.

The morphology of the electrodeposit changes with the electrochemical techniques used. The main techniques are the potentiostatic and the galvanostatic, others are essentially modifications of the last one. If the current is pulsed in the galvanostatic method, we obtain a pulse current plating (PCP) [14]. The two most frequent current profiles in (PCP) are periodically interrupted current (PIC), in which the current is an unidirectional square-wave, and the periodic reverse current (PRC), where a bidirectional square waves is used.

The advantages of the PCP technique [15–18] are:

1. Uniform and dense deposits, fine grains without pores.
2. High deposition rate.
3. Increase of current efficiency and limiting current.
4. Increase of ductility and adherence.
5. Low concentrations of the electroactive species.

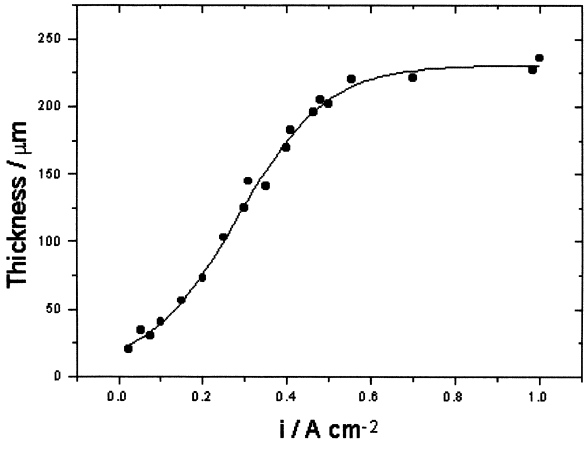

Fig. 4. Thickness variation of the deposits with continuous current density.

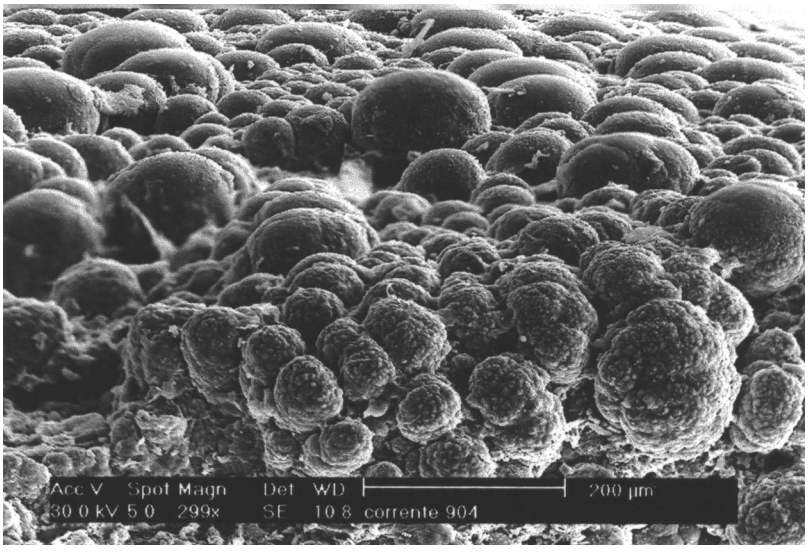

Fig. 5. Micrograph (MEV). Morphology of the continuous current deposit $i = 0.6$ A/cm^2, 20 min and 600°C.

6. Decrease of the anodic effect.
7. Alteration of the morphology.

The experimental (14) parameters of the pulse plating are: the pulse symmetry, anodic and cathodic current density (i_c and i_a), the duration in which the pulses are applied (cathodic time, t_c, anodic time t_a and off time t_{off}) and the pulse frequency.

3. Results and discussion

3.1. Cyclic voltammogram

Previous studies [19] allowed us to establish important experimental conditions for the application of the PCP and the continuous current plating (CCP) techniques. Fig. 1 exhibits at $E = -1.5$ V a cathodic current peak due to the formation of TiB_2 on a copper electrode, for a ratio between B/Ti = 4/1, scan rate of 200 mV/s, at 600°C. The other peaks are due to the oxi-reduction of $K^+ + e^- \rightleftarrows K$ at −2.5 V. On the reversal sweep, in addition to the peak which correspond to the K/K^+ (−2.5 V), there are two other oxidation peaks at about −1.0 and 0.25 V; the first peak (−1.0 V) corresponds to the oxidation of the TiB_2 and the second corresponds to the oxidation of the working electrode (Cu). A distinct behavior was observed [20] for other experimental conditions.

Curve 1 in Fig. 2 depicts the cathodic behavior the system LiF–NaF–KF–0.5 mol/L K_2TiF_6, where peaks 'a' and 'd' correspond to the following two steps Ti(III) to Ti(II) at −0.33 V and Ti(III) to Ti at −1.85 V for the $KTiF_6$ reduction [21]. The small peak before peak d is related to the intermetallic Ti–Pt formation on the working electrode, as have been observed by Makyta et al. [4].

Curve II corresponds to the LiF–NaF–KF–1 mol/L KBF_4 system. It can be seen that the boron reduction, peak 'b', occurs in only one step, B(III) to B at 1.20 V [22]. However, Polyakova et al. [22], in their boron electrodeposition studies have observed two reduction peaks, one of them corresponding to the intermetallic B–Pt formation and the second one to a single step of three electron reduction of boron ions.

Curve III corresponds to the system LiF–NaF–KF–0.5 mol/L K_2TiF_6–1 mol/L, KBF_4, where peak 'c' corresponds to the TiB_2 formation. A depolarization in

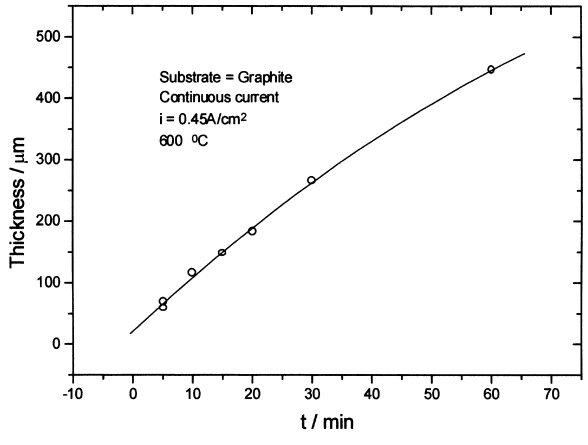

Fig. 6. Thickness variation of the coating with deposition time.

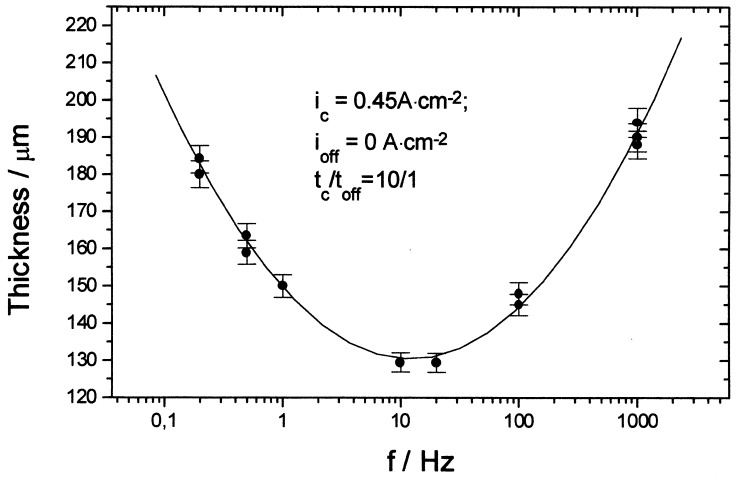

Fig. 7. The thickness variation with the current pulses frequency.

the Ti reduction and a polarization of boron reduction has to occurs simultaneously in order to allow the TiB_2 formation.

The small reduction peak 'f' observed at the same potential of peak 'd', corresponding to the reduction of the remaining Ti which has not reacted with boron. When the ratio B/Ti is 4/1 (Fig. 1), peak f disappears, since all Ti reacts to form TiB_2. In presence of both reactive species, the reduction step Ti (IV → III) was not observed, probably due to a complex formation among the involved electroactive species. Previous studies [20] using the LiF–NaF–KF–1 mol/L K_2TiF_6 system have shown the possible formation of the K_2NaTiF_6 double salt when analyzed via X-ray diffraction (Fig. 3).

3.2. Continuous current density deposition (CCP)

Fig. 4 presents the thickness variation of the TiB_2 deposits on graphite as a function of the applied current density applied, using CCP. When a constant current density is applied for 20 min, the layer thickness grows linearly for values around 0.45 A/cm^2, following therefore, the Faraday's law. At higher current densities, the negative deviation from expected linear dependence can be explained by the formation of a nodular deposit.

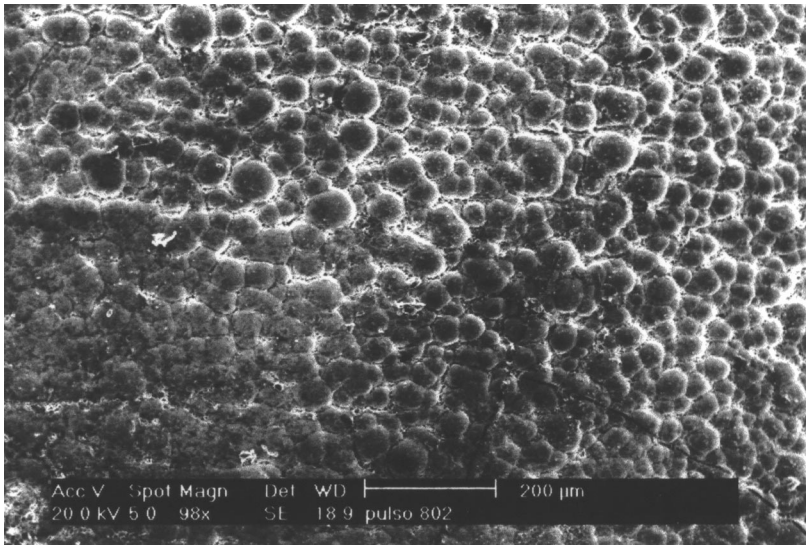

Fig. 8. Micrograph (SEM), frequency 0.5 Hz for i_c = 0.45 A/cm^2, i_{off} = 0 and t_c/t_{off} = 10/1 and 30 min.

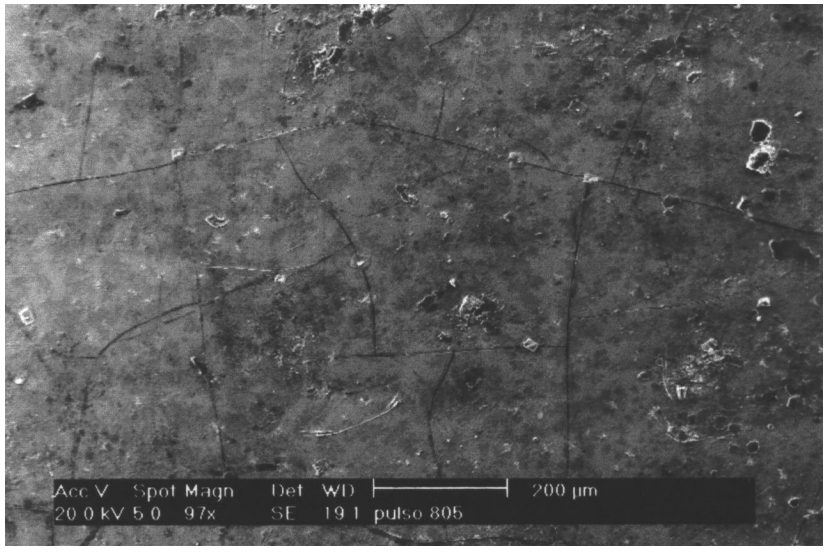

Fig. 9. Micrograph (SEM), frequency 100 Hz for $i_c = 0.45$ A/cm^2, $i_{off} = 0$ and $t_c/t_{off} = 10/1$ and 30 min.

Fig. 5 shows a typical nodular deposit obtained at high current densities at 0.6 A/cm^2 in 20 min. Even so the substrate is well protected by a uniform layer formed before the development of nodules begins.

In Fig. 6, the current density applied was fixed at 0.45 A/cm^2 corresponding to the end of the linear region in the previous experiment increase of the deposition time does not produce thicker deposits as expected, because dendrite and nodule growth adds uncertainties to the thickness measurements.

The pulse current deposition in the experiments clearly improves the quality of the coatings [23], even considering that an important parameter, thickness, exhibits inferior values to CCP.

3.3. Periodically interrupted current (PIC)

3.3.1. Variation of the current pulses frequency

With PIC techniques the thickness variation of the TiB_2 coating with the frequency is presented in Fig. 7 for frequencies between 0.5 and 1000 Hz, current densities $i_c = 0.45$ A/cm^2, fixed from the CCP experiments, $i_{off} = 0.00$ A/cm^2 and for a ratio $t_c/t_{off} = 10$. In the region of decreasing thickness, the deposit exhibits a

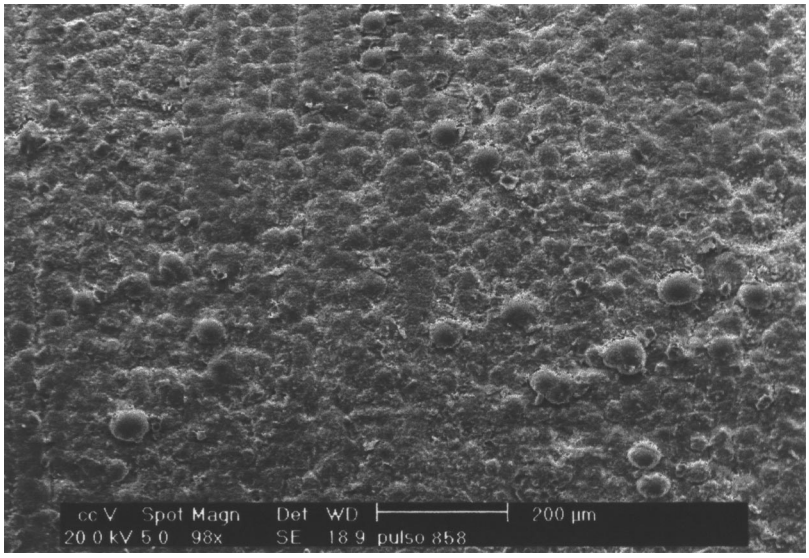

Fig. 10. Micrograph (SEM), frequency 1000 Hz for $i_c = 0.45$ A/cm^2, $i_{off} = 0$ and $t_c/t_{off} = 10/1$ and 30 min.

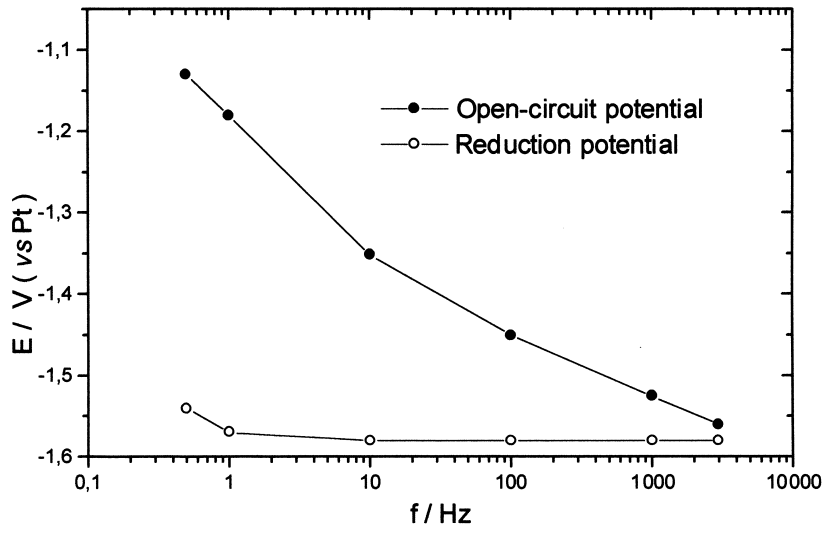

Fig. 11. Open-circuit potential and cathodic potentials resulting from frequency variation (i_{off} = 0 A/cm^2, i_c = 0.45 A/cm^2 and t_c/t_{off} = 1/10).

mixture of nodular, lamellar and dendritic crystallization; as can be seen in Fig. 8 (in spite of some attack caused by the dissolution), suggesting a similar behavior as the one observed in the CCP (Fig. 5).

At frequencies above the minimum of 0.5 Hz, the improvement in the deposit quality is substantial, as can be observed by comparing Figs. 8–10, in spite of the smaller thickness values at 100 Hz.

The nodules are leveled, which produces a metallic brightness. The cracks originate from differences between the thermal expansion coefficients between graphite and the TiB_2 (Fig. 9). The thickness is quite reasonable.

In Fig. 11 it can be observed, that, as frequency increases, the open-circuit potential (i_{off}) and reduction potentials come closer. At low frequencies (0.5 Hz) the deposition potential during a longer period of time, is sufficient to form nodules. The time intervals in which oxidation can occur is insufficient to eliminate them in order to make the coating uniform, even though the potential of the open-circuit is closer to the current oxidation peak presented at the cyclic voltammogram in Fig. 1.

At high frequencies (1000 Hz) the periods between the oxidation and reduction processes are shorter, the deposition potential is reached, while the same does not happen with the oxidation potential presented in the voltammogram of Fig. 1. The obtained deposit is thicker and has more nodules, similar to the one observed in Fig. 8. Using frequencies higher than 2000 Hz the reduction and oxidation potentials are practically identical, looking like those obtained by CCP.

The hexagonal structure [24] of the TiB_2 deposits was identified by X-ray diffraction and the results obtained of the weight percentage of B and Ti in the TiB_2 by X-ray fluorescence are contained in Table 1. No indication of other intennetallic compounds was observed.

The small deviation between the theoretical value, calculated or obtained from the phase diagram (30–31.1%B) [25] and the average of the weight percentage obtained by the X-ray fluorescence can be attributed to the cylindrical surface of the electrode and, mainly, to the fact that boron is a light element, almost at the limit of detection of available equipment.

Between 5 and 100 Hz, smooth deposits without nodules were obtained, 100 Hz corresponding to the thickest coating in otherwise equal conditions. This frequency was chosen for the next experiments.

At low frequencies (Fig. 12a) the TiB_2 deposition potential stabilizes closer to the reduction peak poten-

Table 1
Variation of the weight percentage of Ti and B in TiB_2 in function of frequency

Frequency (Hz)	%B	%Ti
0.5	30.3	69.7
1	36.5	63.5
20	30.5	69.5
100	29.2	70.8
1000	30.4	69.6
Average	31.3	68.6
Theoretical	31.1	68.9

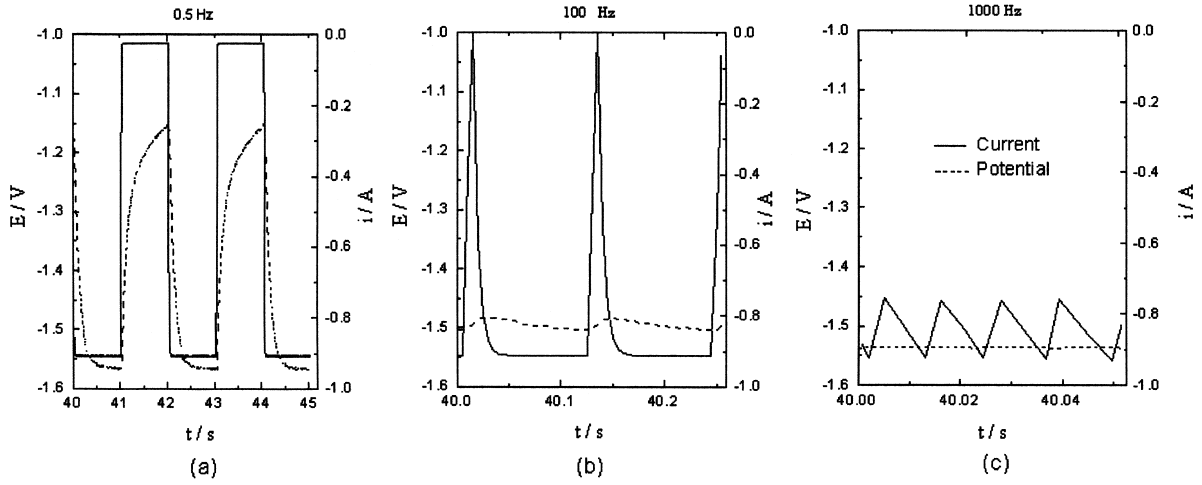

Fig. 12. Effect of PIC frequency on current and potential. $i_c = 0.45$ A/cm^2, $i_{off} = 0$ A/cm^2, $t_c/t_{off} = 10/1$ and 30 min. (a) 0.5 Hz, (b) 100 Hz and (c) 1000 Hz.

tial as shown in the cyclic voltammograms (Figs. 1 and 9), during a long time interval favoring the thickness growing. The oxidation potential reached during the current interruption time ($t_{off} = 5$ s) between the applied pulses is also closer to the oxidation peak potential.

The TiB_2 layer dissolution occurred at ideal conditions but the obtained coating is nodular as depicted in Fig. 8 for 0.5 Hz, because the deposition process occurred in a fashion similar to continuous current plating (Fig. 5).

At intermediary frequencies (Fig. 12b) the TiB_2 deposition potential suffers a fluctuation around the reduction peak potential (Fig. 1) producing only a moderate growth. The oxidation potential reached during the interruption current time ($t_{off} = 2{\cdot}10^{-2}$ s) between the applied pulses is far from the oxidation peak potential Fig. 9. These combined events are enough to flatten the nodular deposit as depicted in (Fig. 9) for 100 Hz.

At high frequencies (Fig. 12c) the short current interruption time ($t_{off} = 3{\cdot}10^{-3}$ s) between the applied pulses causes the TiB_2 deposition potential being constant during the entire process. The TiB_2 oxidation potential that can be reached generally is closer to the deposition potential (Fig. 11) and does not change the

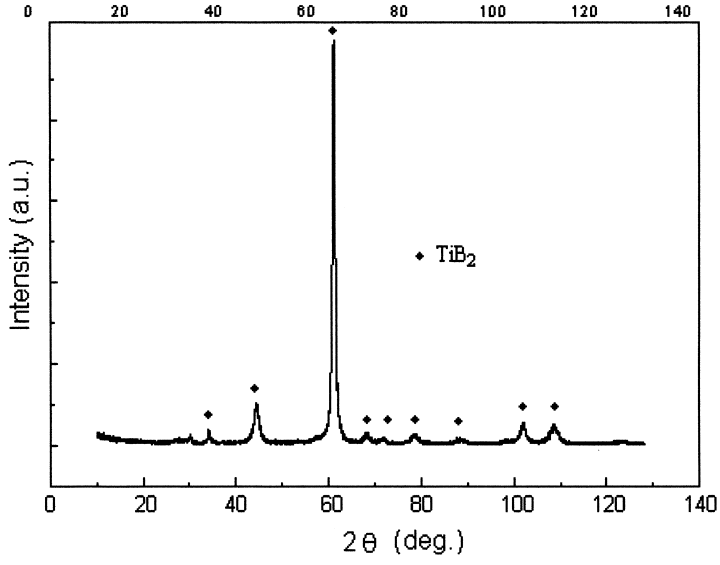

Fig. 13. TiB_2 X-ray diffraction analysis. Frequency 100 Hz for $i_c = 0.45$ A/cm^2, $i_{off} = 0$ and $t_c/t_{off} = 10/1$ and 30 min.

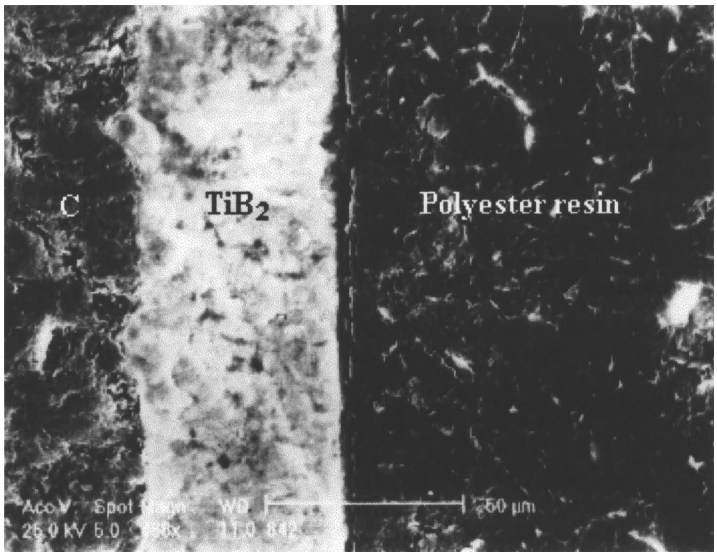

Fig. 14. Cross-section of a titanium diboride coating on graphite substrate. Deposition conditions as in Fig. 13.

morphology of the deposits, resulting in a CCP behavior as can be seen in Fig. 10.

At all applied frequencies the deposits retain the same composition (Table 1) and the presence of TiB_2 phase is shown at the X-ray diffraction (JCPDS No. 35-0741) (Fig. 13). There is practically no growth in coating thickness, but it's quality and substrate adherence are better as is shown in Fig. 14 for a 100-Hz frequency.

3.3.2. Influence of t_c/t_{off} ratio

When the time interval in which the applied current pulse (either cathodic or anodic) has a value not compatible with diffusion coefficient of the ions to be reduced/oxidized, the final result is not acceptable. Therefore, Figs. 15–17 show the influence of t_c/t_{off} on the quality/thickness of the TiB_2 coating. The coating thickness shows only a moderate growth, as can be seen in Fig. 15, confirming the behavior expected and discussed in previous paragraphs.

The quality is very good, with the coating covering the substrate uniformly, without nodules or dendrites, few cracks and high reflectivity, as can be seen (Fig. 16) for a t_c/t_{off} ratio of 3/1. As the variable (t_c/t_{off}) increases, the coating turns opaque and presents some nodule growth, but less accentuated. In Fig. 17, there

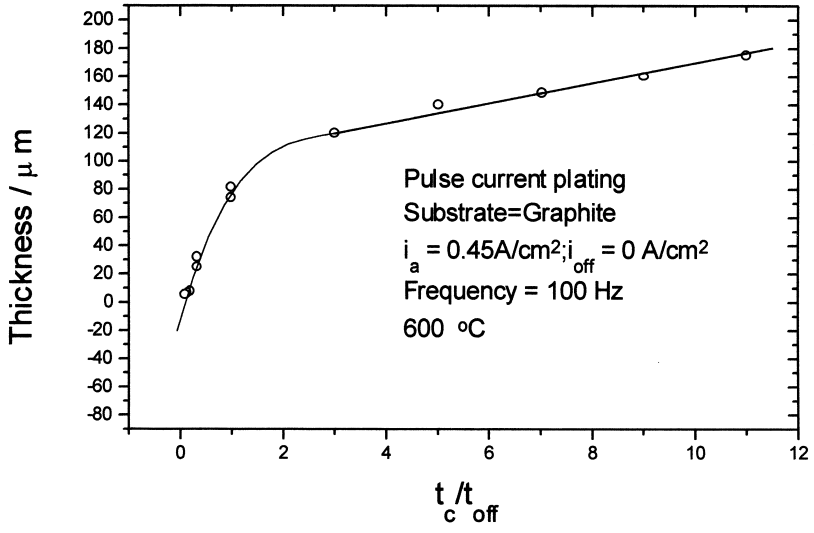

Fig. 15. Influence of t_c/t_{off} ratio over the thickness.

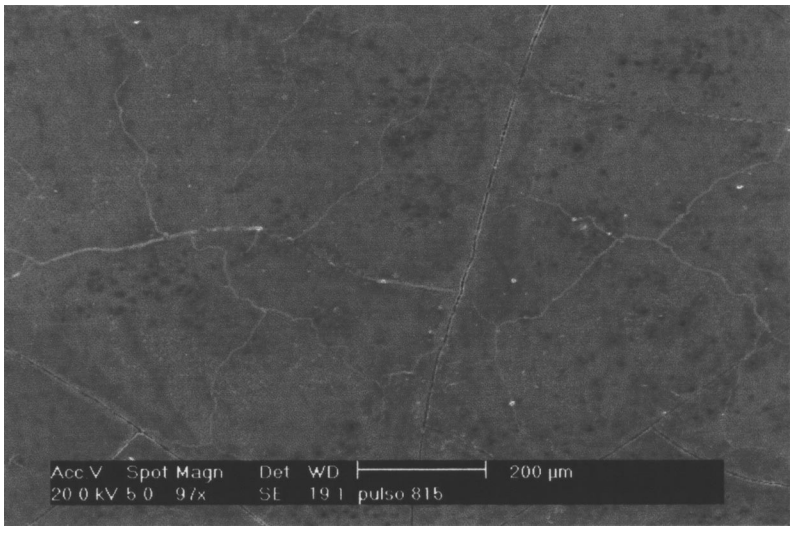

Fig. 16. Micrograph (SEM), for $i_c = 0.45$ A/cm^2, $i_{off} = 0$, $\tau = 30$ min and frequency 100 Hz, $t_c/t_{off} = 3/1$.

is an example of this behavior, closer to the one observed during the CCP.

The t_c/t_{off} chosen for the next experiments was fixed at 5/1, because the layer obtained is thicker than that for the 3/1 ratio and without nodules.

3.4. Periodic reverse current (PRC)

The variation of the applied current densities i_c/i_a with frequency for $t_c/t_{off} = 5$, shows that when the i_c/i_a increases beyond 2, the thickness remains almost constant, as can be seen on Fig. 18.

As the i_c/i_a relation decreases, the dissolution process of the electrodeposited layer increases. The layer thickness decreases together with the existing nodules and dendrites, showing however cracks in the resultant coating (Fig. 19).

Table 2 compares the CCP, PIC and PRC methods used fixing the average current density (0.34 A/cm^2) and the deposition time (30 min) constant for all. (The average current density was established considering interruptions for PIC and subtracting the anodic current for PRC).

The CCP method attains the thickest coating with a characteristic nodular morphology, similar to that depicted at Fig. 5, obtained at high current densities. At low current densities the morphology is similar to that obtained using PIC showed at Fig. 8.

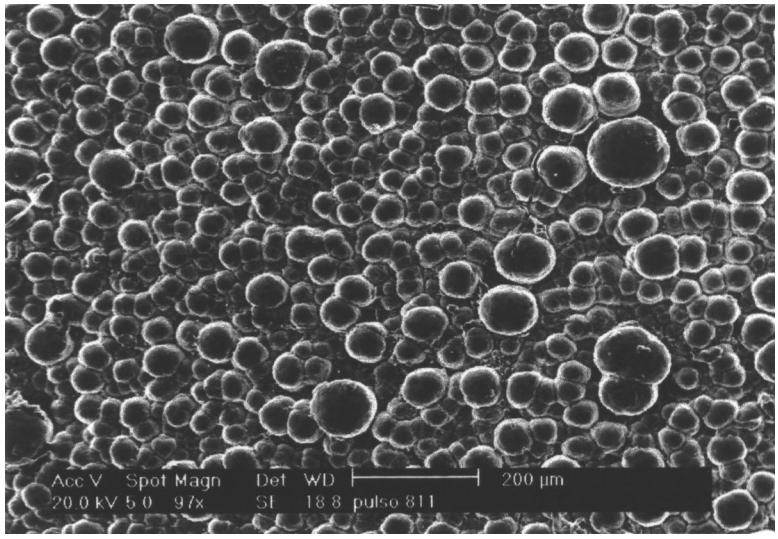

Fig. 17. Micrograph (SEM), for $i_c = 0.45$ A/cm^2, $i_{off} = 0$, $\tau = 30$ min and frequency 100 Hz, $t_c/t_{off} = 11/1$.

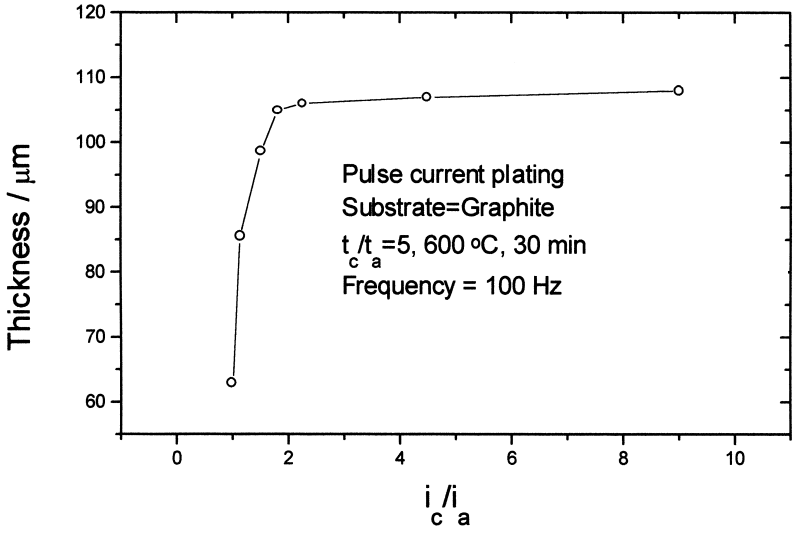

Fig. 18. Variation of the current densities (i_c/i_a) ratio with the TiB_2 coating thickness.

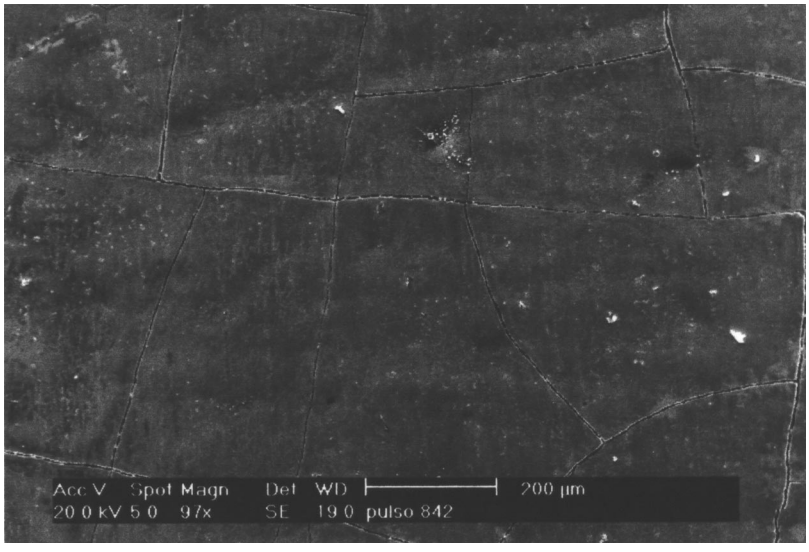

Fig. 19. Micrograph (SEM). Influence of i_c/i_a for $t_c/t_a = 5/1$, $\tau = 30$ min and frequency 100 Hz. $i_c/i_a = 1.8$.

Table 2
Comparison between the three methods (CCP, PIC, PRC)

Method	i (A/cm^2)	Thickness (µm)	Morphology
CCP	0.35	140	nodules
PIC	0.33	120	smooth
PRC	0.33	105	smooth

PIC (Fig. 9) and PRC (Fig. 19) methods do not show differences in morphology; both methods show a smooth deposit surface without nodules, where the coating obtained by the PIC is thicker than that at PRC.

4. Conclusions

1. The electrodeposition with PCP produces coatings with better quality, showing less cracks and better adhesion to the substrate, when compared with those obtained by CCP.
2. The interval of frequencies more suitable for the application of the current pulses is between 5 and 100 Hz; the best thickness obtained was at 100 Hz.
3. The best ratio of the duration of the pulses t_c/t_{off} is between 5/1 and 3/1.
4. The best ratio between the currents iJia is between 1.5 and 1.8.
5. The addition of B ions depolarizes the reduction of the titanium ion and the addition of titanium ions polarizes the reduction of the boron ions resulting in the formation of TiB_2.
6. Even at high current densities no anodic effect was observed, using deposition with current pulse.

Acknowledgements

The authors would like to thank Mr. Celso V. de Morais for the SEM analysis and Vera L.R. Salvador for the X-ray fluorescence analysis. This research was supported by Fapesp through grant No. 96/7923-0 and CNPq (No. 142297/97-6).

References

[1] J.F. Shackelford (Ed.), The CRC Materials Science and Engineering Handbook, 1995.
[2] M.L. Andrieux, Ann. Chim. 12 (1929) 423.
[3] D. Schlain, F.X. McCawley, G.R. Smith, J. Electrochem. Soc. 116 (9) (1969) 1227.
[4] H. Giess, German Patent, 2214633 (1972).
[5] J.D. Kellner, US Patent 3.880.729 (1975).
[6] J. Gomes, K. Uchida, M.M. Wong, Bureau of Mines 8053, 1975.
[7] M. Makyta, K. Gjortheim, M. Matiasovsk, Metall 42 (12) (1988) 1196.
[8] M. Makyta, M. Matiasovský, Electrochim. Acta 34 (6) (1989) 861.
[9] H. Wendt, K. Reuhl, V. Schwarz, Electrochim. Acta 37 (2) (1991) 263.
[10] H. Wendt, K. Reuhl, V. Schwarz, J App. Electrochem. 22 (1992) 161.
[11] M. Makyta, V. Danék, G.H. Haarberg, J. Thonstad, J. App. Electrochem. 26 (1996) 349.
[12] G. Ett, E.J. Pessine, in: III-Congresso Ibero–americano de Engenharia Metalúrgica e de Materiais-IBEROMAT, São Paulo S.P. Brazil, 9–14 October, 1994.
[13] G. Ett, E.J. Pessine, submitted for publication.
[14] C. VanHorn, Metals Handbook, vol. 13, 1986, pp. 282–284.
[15] B.A. Wilson, D.M. Turley, Trans. IMF 67 (1989) 104.
[16] J.C. Vazquez, A.J.B. Dutra, in: XI Congresso Ibero–americano de Electroquímica, Brazil, V25, 694, 1994.
[17] D.M. Soares, Ph.D. thesis, Campinas University, São Paulo, Brazil, 1990.
[18] G. Ett, E.J. Pessine, D.M. Soares, V.L. Salvador, in: 1st Latin-American Interfinish, São Paulo, Brazil, October 9–14, D031, 1997.
[19] G. Ett, E.J. Pessine. X: SIBEE, in: Simpósio Brasileiro de Eletroquímica e Eletroanalítica, São Carlos, SP, Brazil, 1996.
[20] G. Ett, Ph.D. thesis, São Paulo University, to be concluded.
[21] J. de Lepinay, J. Bouteillon, S. Traore, D. Reaud, M.J. Barbier, J. App. Electrochem. 17 (1987) 294.
[22] L.P. Polyakova, G.A. Bukanova, E.G. Polyakov, E. Christensen, J.H. von Barner, N.J. Bjerrum, J. Electrochem. Soc. 143 (10) (1996) 3179.
[23] J. Faucheu, W. Wery, P. Bercot, J. Pagetti, M. Tauchez, in: International Union of Surface finishing — Interfinish 1, 73, 1992.
[24] G. Ett, E.J. Pessine, in: 12° Congresso Brasileiro de Engenharia e Ciências dos Materiais — CBECIMAT. Águas de Lindóia, São Paulo, Brazil, V2, 757, 8–12 December, 1996.
[25] T.B. Massalski (Ed.), Binary Alloy Phase Diagram — ASM International, 2–85, 1990.